

Human peripheral blur is optimal for object recognition

Pramod R T^{1,2*}, Harish Katti^{2*}, & Arun S P^{2,1}

¹Department of Electrical Communication Engineering and

²Centre for Neuroscience

Indian Institute of Science, Bangalore

*Both authors contributed equally to this work

ABSTRACT

Our eyes sample a disproportionately large amount of information at the centre of gaze with increasingly sparse sampling into the periphery. This sampling scheme is widely believed to be a wiring constraint whereby high resolution at the centre is achieved by sacrificing spatial acuity in the periphery. Here we propose that this sampling scheme may be optimal for object recognition because the relevant spatial content is dense near an object and sparse in the surrounding vicinity. We tested this hypothesis by training deep convolutional neural networks on full-resolution and foveated images. Our main finding is that networks trained on images with foveated sampling show better object classification compared to networks trained on full resolution images. Importantly, blurring images according to the human blur function yielded the best performance compared to images with shallower or steeper blurring. Taken together our results suggest that, peripheral blurring in our eyes may have evolved for optimal object recognition, rather than merely to satisfy wiring constraints.

INTRODUCTION

Our vision is sharp at the center of gaze and blurry in the periphery. This is because our retina has a 100-fold increase in photoreceptor density at the centre compared to the periphery (Curcio & Allen, 1990; Curcio, Sloan, Kalina, & Hendrickson, 1990). Why did the retina evolve this way and what are the underlying evolutionary pressures? The prevalent reason attributed to foveation is that it helps to reduce the efferent axonal connections and the burden of processing of orders of magnitude more information that would result from full resolution scenes (Weber and Triesch, 2009).

Here, we propose that foveation may be optimal for object recognition. Our reasoning is as follows: First, we note that object detection is slowed down by clutter as well as by partial matches to target appearance in the background (Katti, Peelen, & Arun, 2017), suggesting that high spatial frequency in the periphery is undesirable. Second, contextual influences play an important role in object detection (Li et al., 2002; Bar, 2004; Davenport and Potter, 2004) and consist of predominantly low spatial frequency information. These two lines of evidence suggest that images should be sampled densely near objects and sparsely in the surrounding context – which is exactly the sampling scheme in the human fovea. If this is true, then it follows that using the human peripheral blur function should yield the best performance, and making this function shallower or deeper should systematically decrease performance.

We tested this possibility using state-of-the-art computer vision algorithms. We selected popular deep neural network architectures and trained them on both full resolution images as well as foveated images. Our main finding is that networks trained on the human peripheral blur profile yielded optimal performance on object detection. This performance was better than that obtained from training on full-resolution images. It was also better than networks trained on shallow and deeper blur profiles, suggesting that the benefit is not a simple consequence of increased salience at the fovea. The gain in performance was the result of

decreased false alarms as well as increase in hit rates, and was evident even from the early epochs of network training. Finally, by analysing spectral content at various distances from objects, we demonstrate that high spatial frequencies are most informative near objects, whereas low spatial frequencies are most informative in the surrounding vicinity. Taken together, our results suggest that human foveation may have evolved for optimal object detection rather than merely due to wiring constraints.

RESULTS

We evaluated the premise that the human peripheral blur function may be optimal for object classification. Figure 1 illustrates how foveation can benefit object detection: when the image is in full resolution (Figure 1A), a deep convolutional network trained on full resolution images correctly identifies the person but makes a false alarm to a traffic cone in the background. In contrast, when the image is foveated on the salient object (in this case, the person; Figure 1B), a deep network trained on these images correctly identifies the person as before but is no longer susceptible to false alarms. Note that since all images are foveated on the foreground object, the location of the foveation by itself is uninformative about object identity. We then compared the performance of convolutional neural networks trained on full resolution with networks trained on foveated images.

Foveation leads to increased objection recognition performance

We systematically created images with varying foveation levels using the human contrast sensitivity function measured at different eccentricities relative to the fovea. To create shallow or extreme foveation levels, we fit the human peripheral blur function to an exponential and increased the spatial decay by a factor of 0.5, 1, 2 or 4 (Figure 2A). Example images created in this manner are shown in Figure 2. A spatial decay factor of 0.5 refers to images blurred with a shallower blur profile compared to that of humans. A spatial decay factor of 1 refers to images blurred according to the human peripheral blur function (Figure 2B). Spatial decay factors of 4 indicates a more extreme blur profile (Figure 2C).

Next we trained a widely used deep convolutional neural network (VGG-16) architecture for 1000-way object classification on the widely used ImageNet dataset (Figure 3A). We trained six separate neural networks where one network was trained on full resolution images (no foveation) and the other five networks were trained on images with different degrees of foveation with spatial decay factors of 0.25, 0.5, 1, 2 and 4 (Figure 3B). We then

tested each network for its generalization abilities by evaluating its accuracy on images never seen during training, but matched to that particular foveation type.

Foveation spatial decay factor	Top-1 accuracy		Top-5 accuracy	
	Train	Test	Train	Test
4	58.9	48.0	81.0	72.0
2	63.4	49.7	83.0	73.4
1 (human)	73.0	52.1	89.0	75.5
0.5	64.8	50.7	84.8	74.0
0.25	61.0	49.0	82.0	72.0
0 (No foveation)	65.9	50.0	84.6	74.0

Table 1. Classification performance of VGG-16 networks on foveated and full resolution images. We report both Top-1 and Top-5 accuracies on both training and test sets. Network trained on foveation level matching the human contrast sensitivity function (foveation spatial decay factor) is highlighted in *red*.

Across all networks, the network trained on images foveated according to the human peripheral blur function gave the best performance (Top-1 accuracy = 52.1% and Top-5 accuracy = 75.5%; Figure 3C; Table 1). This performance was significantly better than networks trained on full-resolution images (Increase in top-1 accuracy: mean \pm std: 2% \pm 0.9% across 1000 categories; $p < 0.000005$, signed-rank test).

Foveation leads to faster learning

In the previous section, we have shown that a CNN trained on foveated images performed significantly better than CNNs trained on other kinds of images. In this section, we explore the nature of this improvement and elucidate other advantages of foveation.

First, we asked if the performance improvement due to foveation was related to a change in the criterion. The network trained on foveated images could be more (or less) conservative compared to the network trained on full resolution images, in which case, both hits and false alarms would decrease (or increase). However, if the representation of various categories is becoming more separable due to foveation, then hits should increase whereas false

alarm should decrease. To test this, we saved the model weights every five epochs during training and calculated hits and false alarms. Specifically, we calculated hits and false alarms over the course of learning for two networks: the best network and the network trained on full resolution images (*no foveation*). We found that the improvement in accuracy for the foveated network largely came from both increase in hits (Figure 4A) and reduction in false alarms (Figure 4B). This trend emerged very early during network training and remained consistent through the course of training. Thus the network trained on foveated images achieves greater accuracy and learns faster.

Evaluation of relevant spatial information

In previous sections, we have shown that a deep neural network trained on images foveated according to the human peripheral blur function achieves optimal classification performance. This raises the intriguing possibility that foveation in the human eye may have evolved to optimize object classification. This evolution may have been driven by a complex CNN-like architecture, or may be the result of even simpler feature detectors. To examine this possibility we asked whether there are asymmetries in discriminative spatial information contained in the low and high spatial frequency bands at the foveal and peripheral locations. Specifically, we hypothesized that the coarser or low spatial frequency information is more discriminative for object identities at peripheral locations and high spatial frequency information is more relevant for foveal locations. If this is true then even simple classifiers based on spatial frequency features could potentially drive the evolution of foveal vision.

To verify this, we selected representative categories from the ImageNet validation dataset and extracted low and high spatial frequency filter responses from each full-resolution image using a multi-scale Gabor filter pyramid (see Methods). We then trained linear classifiers on each band of spatial frequency information present in image patches at various distances

from the centre of the image. We then calculated a modulation index at each eccentricity that indicated the relative importance of low over high spatial frequency content for object recognition defined as $Modulation\ Index = \frac{acc_{hSF} - acc_{lSF}}{acc_{hSF} + acc_{lSF}}$, where acc_{hSF} and acc_{lSF} correspond to decoder accuracy on high and low spatial frequency features respectively. Here we considered features corresponding to only the lowest and highest spatial frequencies for the analysis (and ignored the mid-range frequency features).

We found that the decoder accuracy at all eccentricities was significantly higher than chance level on both low and high frequency features (Figure 5A). Moreover, high spatial frequency features are more informative about the object identity at lower eccentricities as observed by the positive slopes on the blue lines in Figure 5A. We quantified this observation using a modulation index at each eccentricity that captured the improvement in decoder accuracy for high spatial frequency features compared to low spatial frequency features (Figure 5B). The modulation index was positive near the center and negative in the periphery, again showing that high spatial frequencies are more discriminative at the center and low spatial frequencies in the periphery. We conclude that even simple detectors based on spatial frequencies can drive the evolution of foveal vision.

DISCUSSION

Our main finding is that neural networks trained on images foveated according to the human peripheral blur function yield optimal classification performance. This in turn raises the intriguing possibility that foveation in the human eye may be evolved to maximize object recognition performance rather than simply to satisfy wiring constraints. Below we discuss the relation of our findings in the context of the existing literature.

Previous studies have used foveation as a preprocessing step to achieve image compression (Geisler and Perry, 1998) or as a fundamental bottom-up component that guides attention (Itti and Koch, 2001). However, very few studies have explored the computational optimality of foveal and peripheral blur for everyday vision tasks like object recognition. In a recent study, the authors trained object detectors with and without fovea and showed that both detectors showed comparable performance but the foveated detector had significant computational cost savings (Akbas and Eckstein, 2017). This is in contrast to our results where we show significant improvements in object recognition, both in terms of accuracy as well as learning rates. In another study, authors constrained a uniform sampling lattice at the input stage of a deep learning digit detector to have only translatory movements and observed the emergence of a fovea-like lattice pattern after training (Cheung et al., 2016). This also suggests that fovea-like patterns emerge at the input stage of a system due to the statistics of sparse images made up of single handwritten digits at varying scales. We derive similar conclusions from our experiments where we show that the contribution of high spatial frequencies for object recognition is different at foveal and peripheral eccentricities in complex natural images.

Our finding that foveation benefits object recognition raises two important concerns. First, could this benefit be simply due to the target becoming more salient in its surroundings? This is unlikely because this should produce the greatest advantage for extreme foveation, which did not happen in our investigations. Second, how would the visual system know where

to foveate before recognizing an object? There is a large body of evidence suggesting that the primate oculomotor system uses a saliency map to guide saccades. We propose that this saliency map is based on coarse scene contextual information that is available in the visual periphery.

METHODS

Generating foveated images

Any visual stimulus can be analysed in terms of its spatial frequency content with fine details (like edges) attributed to high spatial frequencies and coarse information (like object shape) attributed to low spatial frequencies. The range of visible spatial frequencies is usually measured as the sensitivity to contrast at each spatial frequency and is summarized by the contrast sensitivity function (CSF) which varies as a function of retinal eccentricity (Campbell and Robson, 1968). Based on previous research using grating stimuli for simple detection/discrimination tasks, the contrast threshold for detecting a grating patch of spatial frequency f at an eccentricity e is given by

$$CT(f, e) = CT_0 e^{\alpha f \frac{e+e_2}{e_2}} \quad (1)$$

where f is spatial frequency (cycles per degree), e is the retinal eccentricity (degrees), CT_0 is the minimum contrast threshold, α is the spatial frequency decay constant, and e_2 is the half-resolution eccentricity. This formula has been found to fit published contrast sensitivity data measured in humans under naturalistic viewing conditions (Geisler and Perry, 1998). Although the above formula gives the contrast threshold, what is more important is the critical eccentricity e_c beyond which the spatial frequency f will be invisible no matter the contrast. This critical eccentricity can be calculated by setting the left-hand side of the equation above to 1 and solving for e .

$$e_c = \frac{e_2}{\alpha f} \ln \left(\frac{1}{CT_0} \right) - e_2 \quad (2)$$

The above equation for critical eccentricity (in degrees) was then converted to pixel units by considering the viewing distance. Specifically, critical eccentricity in cm is calculated using the formula

$$e_{c,cm} = d * \tan \frac{\pi e_c}{180} \quad (3)$$

Where $e_{c,cm}$ is the critical eccentricity (in cm) and d is the viewing distance (in cm). This was then converted into pixel units using dot-pitch of the monitor (in cm).

$$e_{c,px} = \frac{e_{c,cm}}{pitch} \quad (4)$$

Then, the input image was low-pass filtered and down-sampled by a factor of two to obtain a lower resolution image. This process of low-pass filtering and down-sampling was repeated up to five times to obtain a sequence of successively lower resolution images. Further, f in the above equation for e_c was set to be the Nyquist frequency at each level of the multi-resolution pyramid and the resulting values of e_c were used to define the foveation regions at each level. That is, pixel values for the foveated image were chosen from different layers of the multi-scale pyramid according to the eccentricity of the pixel from the point of fixation. In our experiments, in addition to using the default values of all the parameters, we obtained different foveation blur profiles by modulating α by a spatial decay factor γ .

$$\alpha_{new} = \alpha\gamma, \quad \gamma = \{0.25, 0.5, 1, 2, 4\} \quad (5)$$

where γ is the spatial decay factor with $\gamma = 1$ being the human foveation blur profile (Equation 1).

CNN training

To test if foveation is computationally optimal for object recognition in natural scenes, we chose ~500,000 images from the ImageNet dataset with manual object level bounding box annotations. We created 5 foveated versions of each image with the point of foveation fixed at the centre of the bounding box and trained deep neural networks for object recognition. Specifically, we used VGG-16 architecture and trained six separate networks (one for the full resolution and five for different foveated versions of the image). Note that, all foveated images were created after scaling the image to 224x224 pixels which is the default size of input to the VGG-16 network. To create images with different levels of foveal blur, we used the equations

described in the previous section. The output of those equations depends crucially on the distance between the observer and the image. How do we find the viewing distance for a CNN? To estimate the optimal viewing distance for the CNN, we trained separate networks on images foveated with a viewing distance of 30, 60, 90, 120 and 150 cm. We found that the CNN trained on a viewing distance of 120 cm yielded maximum performance (data not shown) and hence we have used a viewing distance of 120 cm for all CNN experiments.

For each network, we started with randomly initialized weights and trained the network for 1000-way object classification over 50 epochs of the data with a batch-size of 32. All networks were defined and trained using the PyTorch framework with NVIDIA TITAN-X/1080i GPUs. All the trained models were tested for generalization capabilities on a corresponding test set containing 50,000 images (ImageNet validation set).

Evaluation of spatial frequency content

To verify this, we selected 11 representative categories from ImageNet validation dataset (chosen uniformly from categories 1 through 1000: Tench, Black swan, Tibetan terrier, Tiger beetle, Academic gown, Cliff dwelling, Hook/claw, Paper towel, Slot/one-armed bandit, Water tower, Toilet tissue) and extracted low and high spatial frequency responses using a multi-scale Gabor filter pyramid. Specifically, we rescaled all images to have at least 500 pixels along both dimensions and chose 100 pixels x 100 pixels patches on concentric circles with radii 0, 50, 100, 150 and 200 pixels from the centre of the image. These patches were chosen along 8 equally spaced directions on the circle with the exception of the patch at the centre which was considered only once. We then trained linear object identity decoders at both foveal as well as peripheral locations on the pooled feature representation across all patches corresponding to high or low spatial frequencies. To quantify the importance of high spatial

frequency over low spatial frequency content in object classification, we computed a modulation index defined as

$$\textit{Modulation Index} = \frac{acc_{hSF} - acc_{lSF}}{acc_{hSF} + acc_{lSF}} \quad (6)$$

where acc_{hSF} and acc_{lSF} correspond to decoder accuracy on high and low spatial frequency features respectively.

REFERENCES

- Akbas E, Eckstein MP (2017) Object detection through search with a foveated visual system
Einhäuser W, ed. PLOS Comput Biol 13:e1005743.
- Bar M (2004) Visual objects in context. Nat Rev Neurosci 5:617–629.
- Campbell FW, Robson JG (1968) Application of fourier analysis to the visibility of gratings.
J Physiol 197:551–566.
- Cheung B, Weiss E, Olshausen B (2016) Emergence of foveal image sampling from learning
to attend in visual scenes. arXiv Prepr arXiv161109430.
- Curcio C, Sloan K, Kalina R, Hendrickson A (1990) Human photoreceptor topography. J
Comp Neurol 4:497–523.
- Curcio CA, Allen KA (1990) Topography of ganglion cells in human retina. J Comp Neurol
300:5–25.
- Davenport JL, Potter MC (2004) Scene consistency in object and background perception.
Psychol Sci 15:559–564.
- Geisler WS, Perry JS (1998) Real-time foveated multiresolution system for low-bandwidth
video communication. Proc SPIE 3299:294–305.
- Itti L, Koch C (2001) Computational modelling of visual attention. Nat Rev Neurosci 2:194–
203.
- Katti H, Peelen M V, Arun SP (2017) How do targets, nontargets, and scene context
influence real-world object detection? Attention, Perception, Psychophys.
- Li FF, VanRullen R, Koch C, Perona P (2002) Rapid natural scene categorization in the near
absence of attention. Proc Natl Acad Sci U S A 99:9596–9601.
- Weber C, Triesch J (2009) Implementations and Implications of Foveated Vision. Recent
Patents Comput Sci 2:75–85.

FIGURES

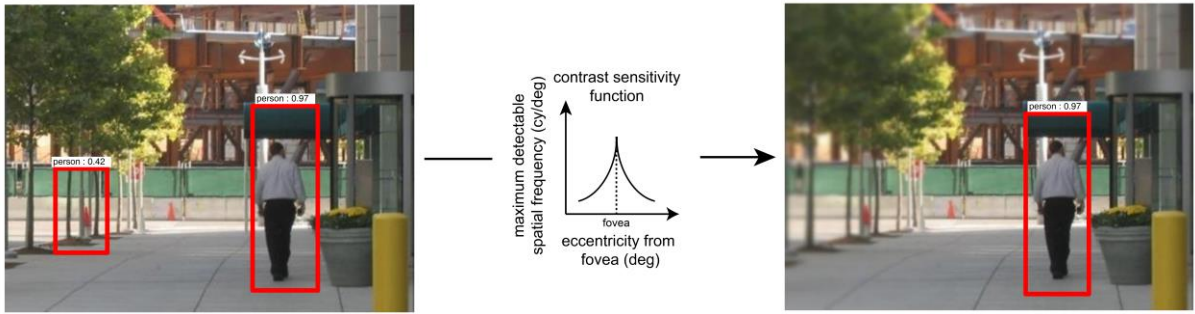


Figure 1 Example full resolution image with object detections showing multiple false alarms (*left*). Object detections on the same image after passing the image through foveation (*right*). We can see that false alarms have greatly reduced. A plot of human contrast sensitivity function used to generate foveated image is shown in the middle. Object detections were generated using an RCNN trained on the PASCAL-VOC dataset.

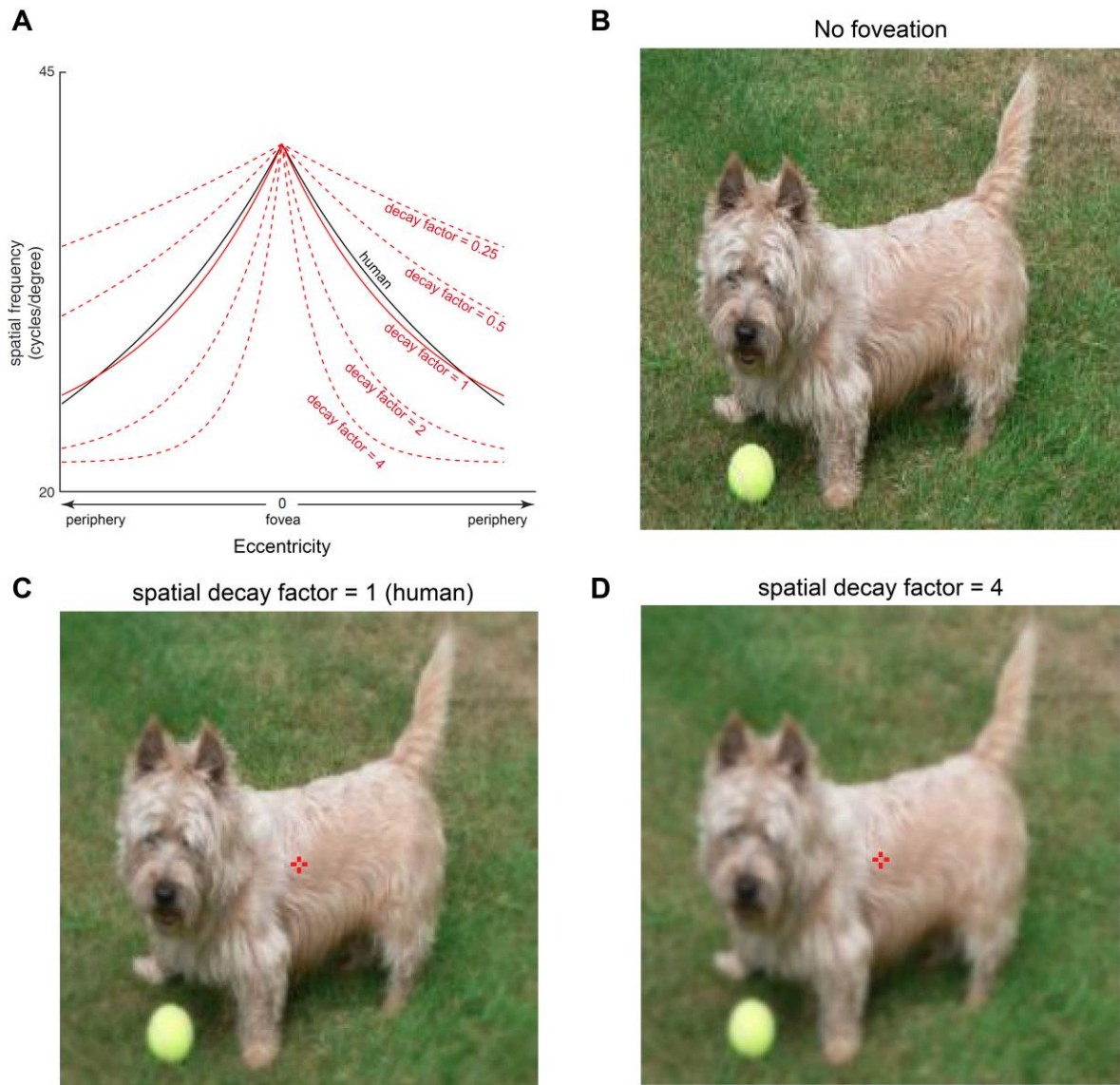


Figure 2. Example foveated images

(A) Human derived contrast sensitivity function (*solid black line*) and the corresponding exponential fit (*solid red line*). The spatial decay of the exponential was varied by scaling the human exponential fit to obtain deviant blur profiles (*dashed red lines*). (B) Example full resolution image; (C) Same as B but foveated with a spatial decay of 1, which corresponds to the human peripheral blur function. Viewed from the appropriate distance, this image will look identical to the full resolution image in B; (D) Same as B but foveated with a more extreme peripheral blur (spatial decay factor = 4).

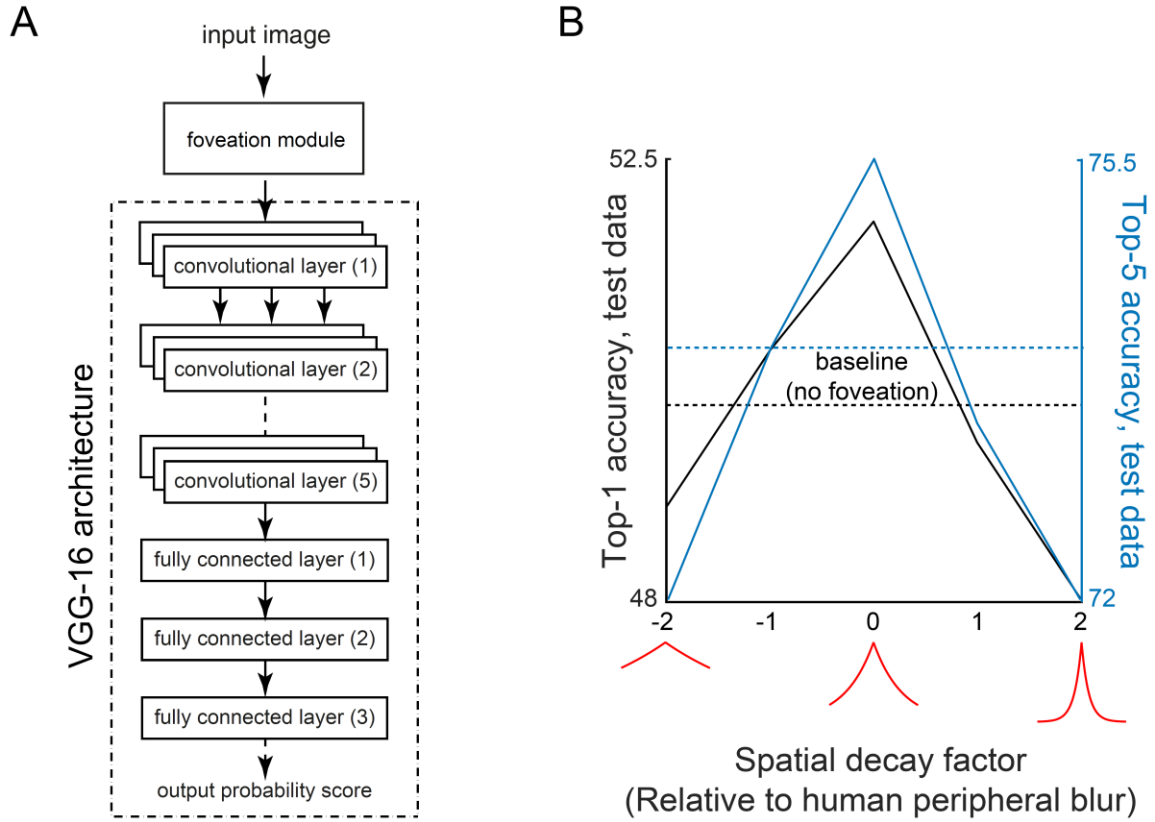


Figure 3 Foveation improves object recognition. (A) Schematic of the VGG-16 neural network architecture; (B) Top-1 (*black*) and Top-5 (*blue*) accuracies of neural networks trained on foveated images with varying degrees of blur. Baseline accuracy in the no foveation case is shown as dotted lines.

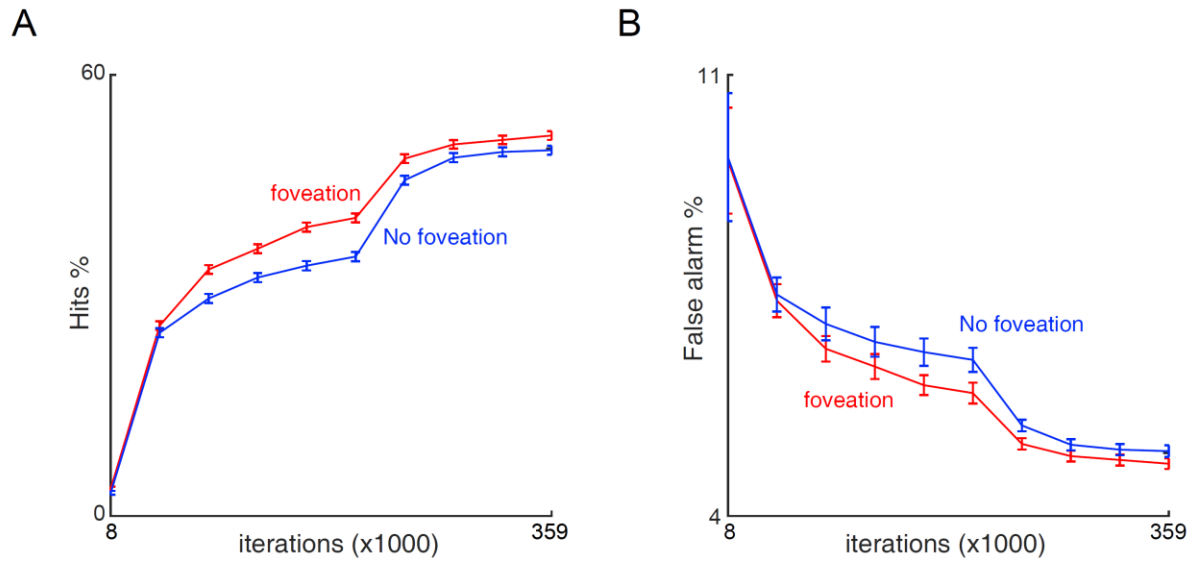


Figure 4 Object recognition performance over the course of training. (A) Plot of percentage hits as a function of learning for networks trained on foveated images (*red*) and full resolution images (*blue*). (B) Same as in (A) but for false alarms. In both plots the x-axis indicates the number of iterations (or batches of data) in multiples of 1000. Error bars indicate s.e.m. across 1000 categories.

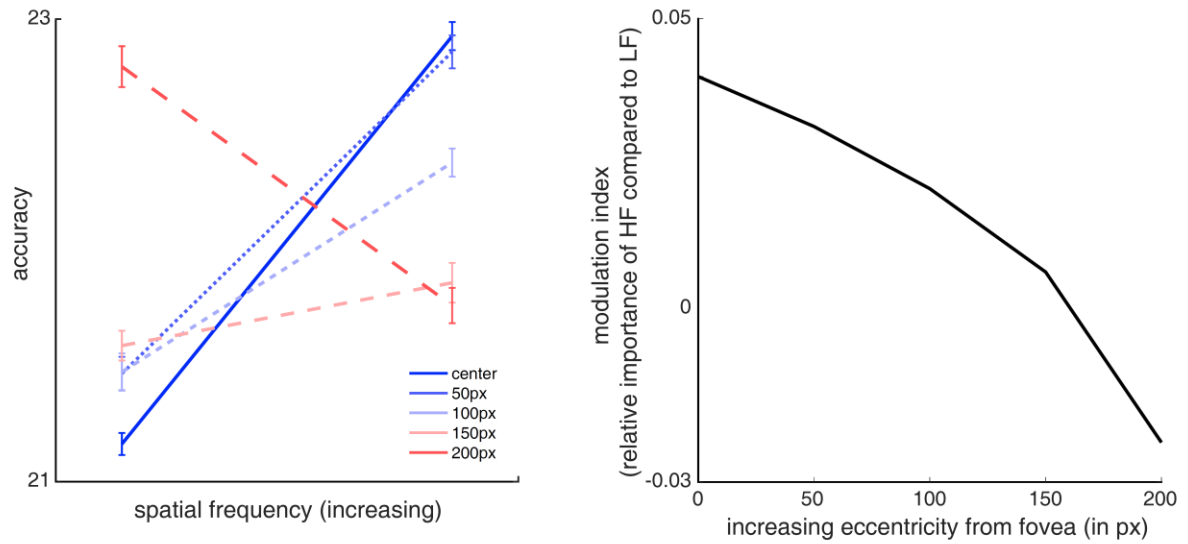


Figure 5 High spatial frequency content is discriminative of object identity at foveal compared to peripheral eccentricities. (A) Accuracy of a 11-way object decoder plotted as a function of spatial frequency for different eccentricities (px is pixels; the shorter dimension of the full image measured 500px). (B) Modulation index showing the relative importance of high compared to low spatial frequency features for different eccentricities.